K_p Forecast Model Using Unscented Kalman Filtering

Charles J. Wetterer[1]

Colorado Professional Resources, LLC supporting SMC SLG/WMLE

Moriba Jah[2]

Air Force Research Laboratory (AFRL)

Kevin Scro[3]

Space and Missile Systems Center (SMC)

CONFERENCE PAPER

The planetary geomagnetic K_p index (3-hour average recorded every 3 hours) exhibits a high degree of correlation from one value to the next. In fact, a simple persistence model that forecasts the next 3-hr value as being equal to the current value shows a linear correlation coefficient of r = 0.797 and a root-mean square error of RMSE = 0.918 from actual values as calculated using historic K_p data from solar cycles 17 through 23. This simple persistence model can be used as a baseline for comparison to other forecast models and, when interpolation effects are taken into account, provides forecasts that are better correlated and have a smaller RMSE to the actual data than most existing neural network methods that use sentinel solar wind and interplanetary magnetic field data. A new forecast method based on the unscented Kalman filter (UKF) is developed to generate forecasts of K_p using previous values of this index to fully exploit persistence and sentinel solar wind interplanetary magnetic field data to provide a geomagnetic storm trigger. The resulting forecast model performs better than all existing K_p forecast models. Model performance is measured by calculating the linear correlation coefficient and the RMSE between the forecast value and the actual value. A new skill score that assesses how well the model predicts the onset of a geomagnetic storm is also introduced. The UKF-based model offers the opportunity for further improvement by adding new inputs and refining the state and measurement functions in the filter and can be used to forecast other geomagnetic indices as well.

1. INTRODUCTION

The three-hour planetary geomagnetic index K_p is one of the most commonly used geomagnetic indices to indicate the severity of global magnetic disturbances. Indeed, the NOAA's Space Weather Prediction Center (SWPC) uses an estimated K_p value to determine their Geomagnetic Storm warnings. References [1] and [2] provide excellent overviews of the origin and use of this index as well as detailed examinations of the precision and accuracy of existing forecast models. Most of these forecast models are based on using a neural network (NN) with sentinel solar wind and interplanetary magnetic field (IMF) derived inputs from the Sun-Earth L1 libration point, with some including the most current estimated K_p measurement as an input as well.

Operations that rely on K_p are challenged continuously to generate creditable forecasts of geomagnetic activity. Before considering transient events that can elevate the level of geomagnetic disturbances, the forecaster establishes a baseline forecast without transient features. Two primary considerations are persistence and recurrence. Persistence assumes what is happening from hour-to-hour or even from day-to-day will not change. Recurrence

[1] Colorado Professional Resources, LLC Chief Scientist, Colorado Springs, Colorado, USA. Subcontract JT515 to TEAS contract FA9200-07-C-0006 on task order TEASV-08-1204

[2] Director, Advanced Sciences and Technology Research Institute for Astrodynamics (ASTRIA), AFRL, Albuquerque, New Mexico, USA

[3] Defense Meteorological Satellite Program Systems Group Technical Director, Peterson AFB, Colorado Springs, Colorado, USA

Report Documentation Page

Form Approved
OMB No. 0704-0188

1. REPORT DATE	2. REPORT TYPE	3. DATES COVERED
SEP 2010		**00-00-2010 to 00-00-2010**

4. TITLE AND SUBTITLE	5a. CONTRACT NUMBER
Kp Forecast Model Using Unscented Kalman Filtering	5b. GRANT NUMBER
	5c. PROGRAM ELEMENT NUMBER
6. AUTHOR(S)	5d. PROJECT NUMBER
	5e. TASK NUMBER
	5f. WORK UNIT NUMBER
7. PERFORMING ORGANIZATION NAME(S) AND ADDRESS(ES) **Air Force Research Laboratory,Advanced Sciences and Technology Research Institute for Astrodynamics (ASTRIA),Kirtland AFB,NM,87117-5776**	8. PERFORMING ORGANIZATION REPORT NUMBER
9. SPONSORING/MONITORING AGENCY NAME(S) AND ADDRESS(ES)	10. SPONSOR/MONITOR'S ACRONYM(S)
	11. SPONSOR/MONITOR'S REPORT NUMBER(S)

12. DISTRIBUTION/AVAILABILITY STATEMENT
Approved for public release; distribution unlimited

13. SUPPLEMENTARY NOTES
2010 Advanced Maui Optical and Space Surveillance Technologies Conference, 14-17 Sep, Maui, HI.

14. ABSTRACT

15. SUBJECT TERMS

16. SECURITY CLASSIFICATION OF:			17. LIMITATION OF ABSTRACT	18. NUMBER OF PAGES	19a. NAME OF RESPONSIBLE PERSON
a. REPORT	b. ABSTRACT	c. THIS PAGE			
unclassified	**unclassified**	**unclassified**	**Same as Report (SAR)**	**10**	

assumes no change from one solar rotation to the next. Even though the Sun is a dynamic main sequence star, the time scale of changes allows both persistence and recurrence to be useful forecast agents.

In this paper, we will follow this example by establishing a baseline forecast in the absence of transient events using persistence alone and then add sentinel solar wind inputs to forecast the onset of geomagnetic storms. First, an analysis of historic values of K_p from solar cycles 17 through 23 is accomplished and a simple persistence model and an average persistence model are developed to establish baseline forecasts of future values of K_p from the current nowcast value alone. These models will be the standard by which to evaluate the performance of the existing NN sentinel models. The effects of the data sets used and how that affects the measured performance of the particular forecast models will also be taken into account. A new skill score that assesses how well the model predicts increases in activity during geomagnetic storms is also introduced. Next, the unscented Kalman filter (UKF) [3] is described and used to create a new mechanism for forecasting future values of K_p. The UKF combines Kalman filtering, the optimal filter for estimating linear systems, with the unscented transform, which uses deterministic sampling to estimate the state and covariance of the system through a nonlinear function. The UKF has seen extensive use in spacecraft attitude determination [4,5,6,7]. The UKF model forecasts will first exploit persistence alone and then incorporate sentinel solar wind data as a storm-time trigger. Again, model performance is evaluated by calculating the linear correlation and root-mean square error between the forecast K_p and the actual K_p, and the storm-time onset skill score and comparing with the performance of the simple and average persistence models.

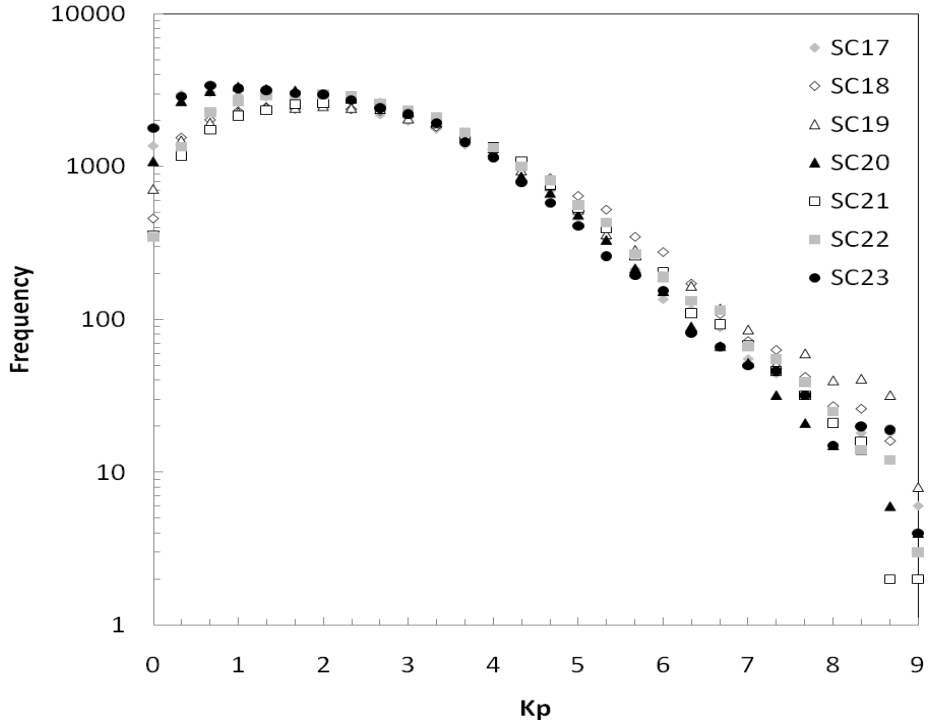

Fig. 1. Frequency of three-hour K_p during different solar cycles. Open symbols are 10-year cycles, gray symbols are 11-year cycles, and solid symbols are 12-year cycles.

2. HISTORIC K_p FROM SOLAR CYCLES 17 THROUGH 23

The three-hour planetary K_p index were tabulated by solar cycle using the archives at the World Data Center for Geomagnetism, Kyoto (http://swdcwww.kugi.kyoto-u.ac.jp/index.html). Fig. 1 displays the distribution of K_p during each of the seven solar cycles covered. The 12-year solar cycles (SC20, SC23) show a higher frequency of low geomagnetic activity ($K_p < 2$) and a lower frequency of moderate to high geomagnetic activity ($K_p > 5$) as compared to the 10-year solar cycles (SC18, SC19, SC21). The 11-year solar cycles (SC17, SC22) fall somewhere in between. Fig. 2 displays the root mean square error (RMSE) of each K_p with past values as a function of time.

Clearly evident is a dip at 27 days indicating solar feature recurrence consistent with the Carrington synodic rotation period of the Sun where the same active region or coronal hole/high speed stream produces similar solar wind and interplanetary magnetic field conditions and thus similar geomagnetic conditions and variations. The most recent past values representing persistence, however, provide a lower RMSE and are thus more predictive to estimating future values.

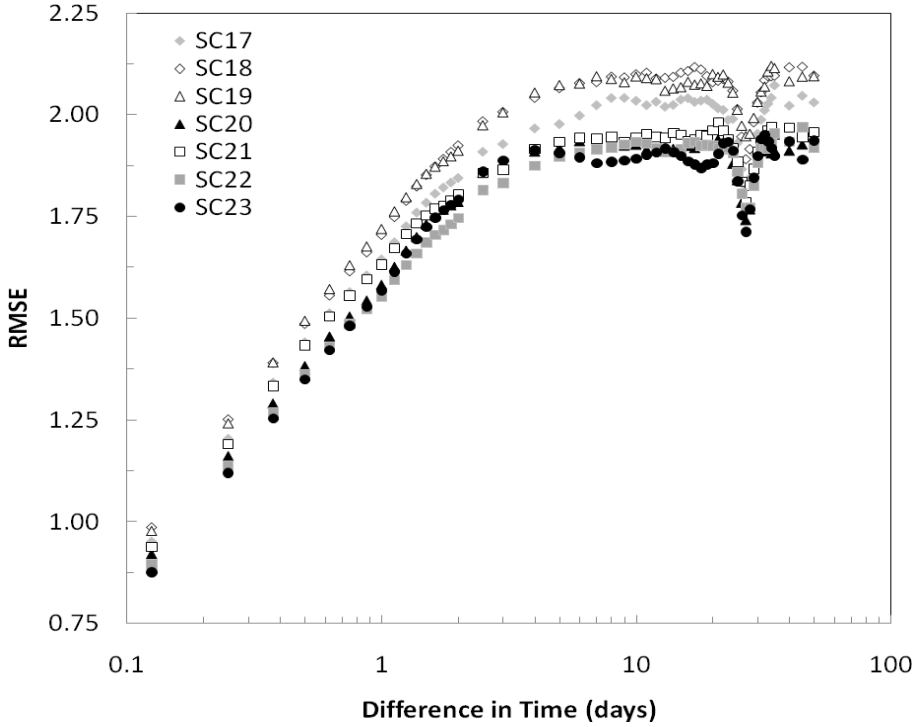

Fig. 2 – RMSE of difference of K_p with past values for different solar cycles.

3. THE K_p SIMPLE AND AVERAGE PERSISTENCE MODELS

Models based on the nowcast K_p will be evaluated to form a baseline to compare all other forecast models. In light of Fig. 2, the K_p simple persistence model uses the nowcast K_p as the forecast for the next K_p and the K_p average persistence model uses the average of the next value from the historic data with the same nowcast K_p as the forecast for the next K_p. Fig. 3a shows the results of running the models on all the data (3 hour time interval) to provide a forecast 3 hours ahead. Fig. 3b shows the RMSE in the predicted values as a function of the actual K_p values. There is an improvement in the overall RMSE from actual values when comparing the average persistence model over the simple persistence model. This improvement is due to the marked improvement in RMSE for K_p values close to the modal value at the expense of the RMSE away from the modal value as displayed in Fig. 3b. The 3-hour forecast correlation coefficients and overall RMSE for the simple persistence model are listed in Table 1 for each solar cycle, two sets of data used with the UKF models (1933-2008 and 1998-2008) and the data sets of [1,8,9] (1975-2001) and [2] (April 2001, all of 2006 and 2007). The test set for [10], described below, is identical to Solar Cycle 22.

The persistence correlation coefficient for a 3-hour forecast is about r = 0.8 for all time periods. Most of the previous forecast models described in the literature, however, generate K_p forecasts of less than 3 hours. These models are their reported results are summarized in Table 2. To implement and evaluate these models using a nowcast K_p, it is either necessary to create a new set of K_p data, for example by interpolating between the official 3 hour values (to a 15 minute time granularity as done in [1]) or use a different source of data (the estimated 3-hour K_p that is calculated hourly by the Air Force Weather Agency (AFWA) Space Weather Operations Center as suggested by [2]). Both options affect the resulting correlation coefficients and must be understood before direct comparison to the persistence models can be made. Interpolating between points artificially enhances the correlation by de-emphasizing extreme values in the time series and will increase the correlation and decrease the RMSE. For hourly

sampling of a 3-hour smoothed value, the correlation will increase and RMSE will decrease because a direct dependence between the hourly values has been added due to the smoothing process.

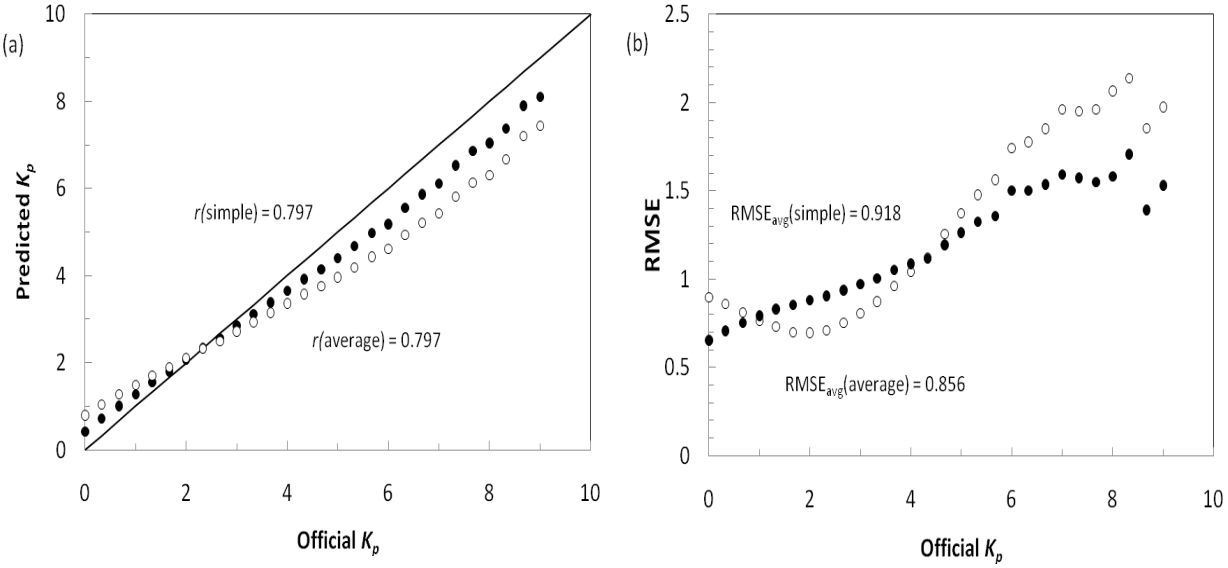

Fig. 3 –K_p simple persistence model (solid circles) and K_p average persistence model (open circles) 3-hour ahead performance. (a) predicted versus actual and (b) RMSE

Table 1. 3-hr forecast correlation coefficient for simple persistence model

Time period	r	RMSE
SC17	0.793	0.946
SC18	0.791	0.985
SC19	0.793	0.977
SC20	0.784	0.922
SC21	0.779	0.938
SC22 [10]	0.801	0.894
SC23	0.810	0.876
1933-2008 (data set 1)	0.797	0.933
1998-2008 (data set 2)	0.812	0.878
1975-2001 [1,8,9]	0.793	0.913
Apr 2001, 2006-2007 [2]	0.806	0.809

Care must be taken when using hourly data (whether estimated or interpolated) of this 3-hour average to compare the baseline results of the K_p persistence models to another forecast model. Nevertheless, Fig. 4 attempts to do just this by comparing the previous published model linear correlation coefficients and RMSE with the K_p simple persistence model. Two sets of results from the K_p simple persistence model are displayed: the first (solid line) using the official K_p from 1933-2008 in the original 3-hr granularity oversampled to a 1-hr granularity (the K_p reported for a particular 3-hour window was taken to be the K_p for each hour in that 3-hour window); the second (dashed line) using this same data interpolated to a 1-hr granularity. Oversampling avoids the boost in correlation that results by interpolating.

The Costello NN [8], NARMAX [9], and APL models [1] results in Table 2 are taken from [1] using 15-minute interpolated official K_p from 1975-2001 and is best compared to the dashed line. The RMSE values were not reported in [1] and were instead estimated using their Figs. 1, 2, 3, 6a, 7a and 8. Reference [10] (BWL in Table 2) NN model test data are official K_p values at the original 3-hour tempo from SC22 (1986-1996) and is best compared to the solid line. Reference [2] (BRL in Table 2) linear models and NN models use the official K_p from April 2001 and 2006, 2007 transformed to a 1-hour cadence by oversampling and are best compared to the solid line. In all but one case, use of the sentinel solar wind and IMF inputs does not improve the overall correlation between the actual

values and the forecast values from using past values alone as in the K_p persistence models described above. In all cases, the RMSE is not improved. Due to the high degree of persistence in K_p, evaluating models with a skill score that uses all data (e.g. Figs. 9 and 10 in [1] and Fig. 13 in [2]) shows similar results when comparing existing NN model results to simple persistence. Using these measures as a basis of forecast performance are not adequate and a new measure that evaluates how well the model forecasts the onset of a geomagnetic storm is required.

Table 2. K_p forecast model descriptions

Name	Input	Forecast (hrs)	r	RMSE	Reference
Costello NN	v, B_z, $\|\mathbf{B}\|$	1	0.75	0.71	[8,1]
BWL NN	v, n, B_z, $\|\mathbf{B}\|$	1	0.768	0.985	[10]
NARMAX	v, p, B_z, $\|\mathbf{B}\|$, K_p	1	0.77	0.79	[9,1]
APL Model 1	v, n, B_z, $\|\mathbf{B}\|$, K_p	1	0.92	0.55	[1]
APL Model 2	v, n, B_z, $\|\mathbf{B}\|$, K_p	4	0.79	0.97	[1]
APL Model 3	v, n, B_z, $\|\mathbf{B}\|$	1	0.84	0.85	[1]
BRL linear 1-hr	BI	1	0.712	1.44	[2]
BRL linear 3-hr	BI	3	0.770	1.21	[2]
BRL NN Model 1	BI, K_p	1	0.863	0.71	[2]
BRL NN Model 2	BI, K_p	2	0.854	0.82	[2]
BRL NN Model 3	BI	1	0.852	1.12	[2]
BRL NN Model 4	BI	3	0.845	1.12	[2]

v, p, n = solar wind speed, dynamic pressure, density
$|\mathbf{B}|$ = IMF magnitude
B_z = z-component of IMF
BI = Boyle Index (derived from v, $|\mathbf{B}|$, and B_z) see [2])
K_p = nowcast K_p value

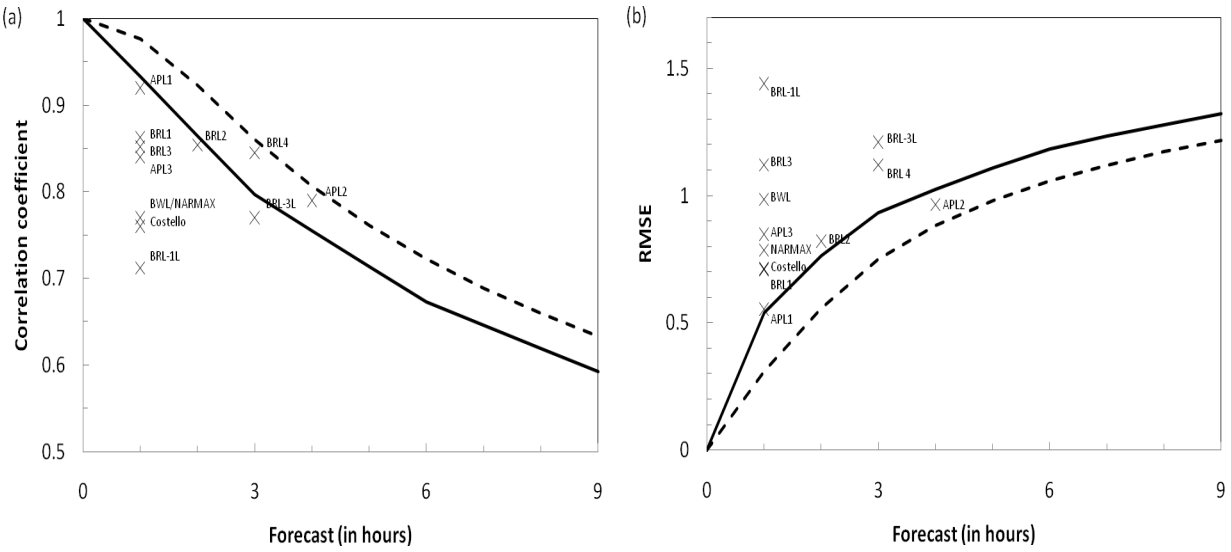

Figure 4 –K_p simple persistence model x-hour ahead (a) correlation coefficient and (b) RMSE as a function of x (forecast in hours) for all data (solid line are original 3-hr oversampled at 1-hr granularity and dashed line for original data interpolated to 1-hr granularity). Previously published model results plotted as reported for comparison.

To this end, a skill score based on the Heidke Skill Score (Eq. 1 in [2]) will be used to evaluate the forecast models. In this skill score, only those times when the actual value exceeds a "storm threshold" will be evaluated. A "hit" (a)

is when $(K_p)_{i+1} \geq (K_p)_i + T$ and $(\tilde{K}_p)_{i+1} \geq (K_p)_i + T - S$, a "miss" (c) is when $(K_p)_{i+1} \geq (K_p)_i + T$ and $(\tilde{K}_p)_{i+1} < (K_p)_i + T + S$, a "false positive" (b) is when $(K_p)_{i+1} < (K_p)_i + T$ and $(\tilde{K}_p)_{i+1} \geq (K_p)_i + T - S$, and a "correct rejection" (d) is when $(K_p)_{i+1} < (K_p)_i + T$ and $(\tilde{K}_p)_{i+1} < (K_p)_i + T + S$, where K_p is the actual value, $\tilde{K}_p$ is the forecast value, *T* is an "increase threshold" corresponding to the change in K_p required for the onset of a geomagnetic storm and *S* is a "tolerable error" in forecasting the magnitude of the onset. By this measure, simple and average persistence have a storm onset skill score for a +3 hour forecast of SS = 0, for storm threshold of K_p = 3.9, *T* = 1.0, and *S* = 0.4.

4. THE UKF FORECAST MODEL

The Kalman filter will be used to generate a forecast for K_p. The basic steps in a Kalman filter are: 1. the state vector and covariance from the current time step are passed through a state function that translates the values to the next time step creating an "a priori" state vector and covariance, 2. the "a priori" state vector and covariance are used in a measurement function that translates the values to a corresponding predicted measurement and covariance, 3. the predicted measurements and covariance are then compared to the actual measurements and covariance at that time step and this difference along with the so-called "Kalman gain" are used to adjust the values in the a priori state vector and covariance to an "a posteriori" state vector and covariance, and 4. this a posteriori state vector and covariance are then used at the start of the next step. The predicted measurement in step 2 can be used as a forecast value and repeated use of the state and measurement functions at this point in the Kalman filter cycle can create forecasts any number of time steps into the future for the current step.

In a regular Kalman filter, the state function and measurement function must be linear. Various methods have been employed to extend the Kalman filter for use with nonlinear functions. We will use the Unscented Kalman Filter (UKF) (also called the Sigma-Point Kalman Filter) that employs the unscented transform [3]. In this study, we use the nomenclature of [5] and set the UKF tuning parameters to $\alpha = 1, \beta = 0$ and $\kappa = 0$.

The key to using the UKF as a forecast model will be in creating a state vector ($\hat{x}_k$) and covariance (P_k), a state function ($f(\hat{x}_k, w_k)$) and a measurement function ($h(\hat{x}_k, v_k)$). In each of the models described below, we use an n×1 state vector given by

$$\hat{x}_k^+ = \vec{c}_k^+ \tag{1}$$

where $\vec{c}_k^+$ is a vector of parameters to be used in the measurement function. The noiseless state function used will be

$$\hat{x}_{k+1} = f(\hat{x}_k, 0) = \hat{x}_k \tag{2}$$

which simply means the parameters in the state vector are assumed to be constant within the time step.

Three different noiseless measurement functions that forecast K_p will be evaluated:

$$\tilde{y}_k = h(\hat{x}_k, 0) = \vec{A}_k^T \cdot \hat{x}_k \tag{3a}$$

$$\tilde{y}_k = h(\hat{x}_k, 0) = \vec{A}_k^T \cdot \vec{\vec{B}}_k \cdot \vec{A}_k \tag{3b}$$

$$\begin{aligned}\tilde{y}_k &= h(\hat{x}_k, 0) = (\hat{x}_k)_1 + (\hat{x}_k)_2 \cdot (K_p)_k \\ &+ (\hat{x}_k)_3 \log_{10}[(\hat{x}_k)_4 (1 + (\hat{x}_k)_5 n_k)(v_k - (\hat{x}_k)_6)^{(\hat{x}_k)_7} \\ &+ (\hat{x}_k)_8 (B_k - (\hat{x}_k)_9)^{(\hat{x}_k)_{10}} \sin^{(\hat{x}_k)_{11}}\left(\arccos\left(\frac{((B_z)_k - (\hat{x}_k)_{12})}{(B_k - (\hat{x}_k)_{13})}\right) \Big/ 2\right)\end{aligned} \tag{3c}$$

where

$$\vec{A}_k = \begin{bmatrix} 1 \\ (K_p)_k \\ (K_p)_{k-1} \\ \vdots \\ (K_p)_{k-n'+1} \end{bmatrix} \tag{4a}$$

$$\vec{\vec{B}}_k = \begin{bmatrix} (c_k^+)_1 & (c_k^+)_2 & (c_k^+)_3 & \cdots & (c_k^+)_{n'+1} \\ 0 & (c_k^+)_{n'+2} & (c_k^+)_{n'+3} & \cdots & (c_k^+)_{2n'+1} \\ \vdots & \vdots & \ddots & \cdots & \vdots \\ 0 & 0 & 0 & (c_k^+)_{n-2} & (c_k^+)_{n-1} \\ 0 & 0 & 0 & 0 & (c_k^+)_n \end{bmatrix} \tag{4b}$$

The first two measurement functions (Eq. 3a and 3b) will explore the limits of using persistence alone and have a state vector with $n = n' + 1$ and $n = (n'+1)(n'+2)/2$ parameters respectively. The third measurement function (Eq. 3c) will incorporate a quiet time forecast using simple persistence (first two parameters) and a storm trigger using a Boyle index-like function (the remaining eleven parameters) that incorporates sentinel solar wind number density (n_k) and velocity (v_k) and IMF strength (B_k) and z-component ($(B_z)_k$).

The +3hr forecast at step k is $\hat{y}_k$ in the nomenclature of the UKF. Additional forecasts (for +6hr, +9hr, etc…) at step k are accomplished by using Equation 2 and 3a, 3b, or 3c iteratively at that point in the UKF cycle. The values of the solar wind and IMF values used in Eq. 3c for these extended forecasts were kept constant.

In this study, the initial state was set to

$$\hat{x}_0^+ = \begin{bmatrix} 0 & 1 & 0_{1\times(n-2)} \end{bmatrix}^T \tag{5a}$$

$$\hat{x}_0^+ = \begin{bmatrix} \frac{-12.55}{2} & \frac{1}{2} & \frac{8.93}{2} & 10^{-4} \cdot 10^{\frac{-12.55}{8.93}} & 0 & 0 & 2 & 11.7 \cdot 10^{\frac{-12.55}{8.93}} & 0 & 2 & 0 & 0 & 3 \end{bmatrix}^T \tag{5b}$$

The persistence only values (Eq. 5a) correspond to simple persistence while the storm-trigger values (Eq. 5b) correspond to an average of simple persistence and the linear fit to the logarithm of the Boyle index (Eq. 2 in [2]). The components of the covariance matrix associated with the parameters are initially set high to allow the UKF room to adjust them accordingly.

The persistence only measurement functions used K_p data from 1933 through 2008 while the storm-trigger measurement function used K_p data from 1998 to 2008 and corresponding solar wind and IMF data from the Advanced Composition Explorer (ACE). The solar wind and IMF hourly data were tabulated using the Level 2 On-line data archives at the ACE website (http://www.srl.caltech.edu/ACE/ASC/level2/index.html). Any missing hourly ACE data was replaced with the last valid value for that quantity and then averaged to the same 3-hour cadence as the K_p data. All the data was processed with the UKF multiple times using the final state vector of the current iteration as the initial state vector of the next iteration until the resulting linear correlation coefficient from one iteration to the next remained essentially constant. In this way, the final iteration starts with parameter values close to their optimal values. The UKF model performance is measured from this final iteration. Conversely, as done with neural network forecast models, a training data set could have been used to first find these optimal parameters with a test data set then used only once to measure the model performance. This was done for the persistence only models described below where the training data set covered the first solar cycle and the test data set covered the remaining solar cycles and identical results were found.

Various persistence only models with $n' = 1$ to 10 were evaluated. For measurement function Eq. 3a and $n' = 1$, the performance is essentially identical to the average persistence model described in section 3. Increasing n' improved the linear correlation and RMSE slightly indicating some memory in the magnetosphere to past K_p values. Above $n' > 7$, the improvement in performance is negligible. For measurement function Eq. 3b, again the performance improves slightly for greater values of n' and at a faster rate than with Eq. 3a, indicating nonlinear dependencies. Above $n' > 4$, the improvement in performance was negligible and in fact actually became worse above $n' = 6$. The UKF persistence only model will use the results of Eq. 3b with $n' = 4$ in the remaining discussion and figures. All the state vector parameters vary relatively smoothly about nonzero averages. Interestingly, many of the parameters exhibit variations correlated with the solar cycle. The resulting linear correlation coefficients are r = 0.803, 0.688, and 0.613 for a +3 hour, +6 hour, and +9 hour forecast respectively. This represents a 0.8%, 2.2%, and 3.3% improvement over the simple persistence model. The root mean square errors are RMSE = 0.844, 0.996 and 1.059 for a +3 hour, +6 hour, and +9 hour forecast respectively. This represents an 8.0%, 14.0%, and 17.7% improvement over the simple persistence model and a slight improvement over the average persistence model. The storm onset skill score for a +3 hour forecast is SS = 0.017 (for storm threshold of $K_p = 3.9$, $T = 1.0$, and $S = 0.4$), again representing a slight improvement over simple persistence, but essentially a negligible forecast of storm onset.

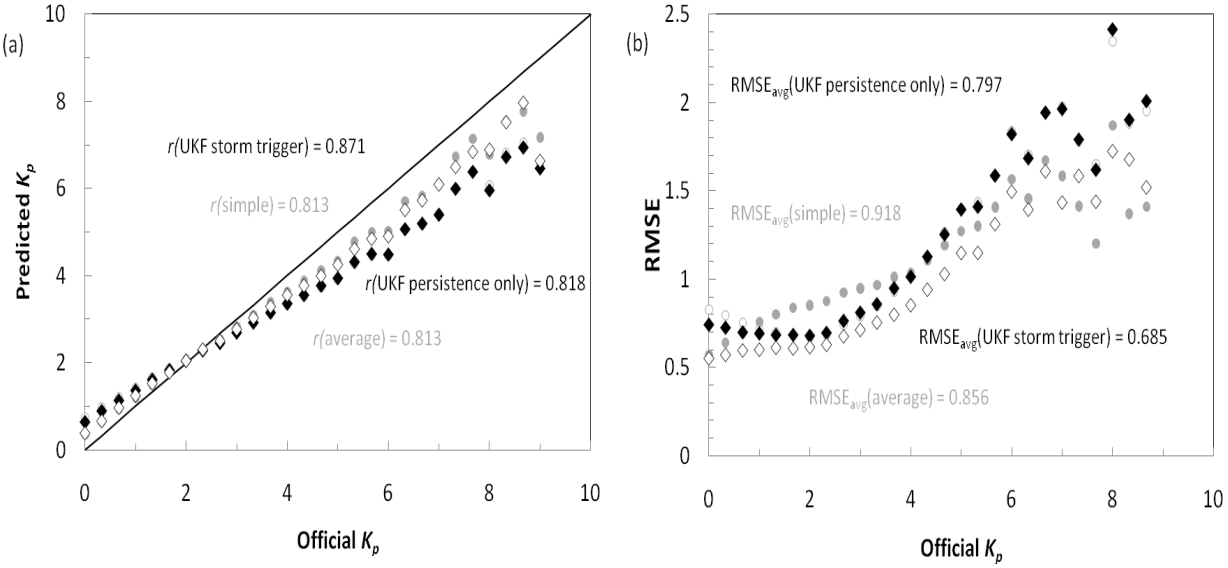

Figure 5 – UKF persistence-only model (solid diamonds) and UKF storm-trigger model (open diamonds) 3-hour ahead performance. (a) predicted versus actual and (b) RMSE. The simple persistence model (closed gray circles) and average persistence model (open gray circles) also shown for comparison.

The storm-trigger model of Eq. 3c improves the forecast significantly. The linear correlation coefficients are r = 0.871, 0.753, and 0.669 for a +3 hour, +6 hour, and +9 hour forecast respectively representing a 7.2%, 8.4%, and

8.4% improvement over the simple persistence model. The root mean square errors are RMSE = 0.685, 0.930, and 1.067 for a +3 hour, +6 hour, and +9 hour forecast respectively representing a 20.4%, 14.9%, and 12.2% improvement over the simple persistence model. Most significantly, the storm onset skill score for a +3 hour forecast is SS = 0.419 (for storm threshold of K_p = 3.9, T = 1.0, and S = 0.4).

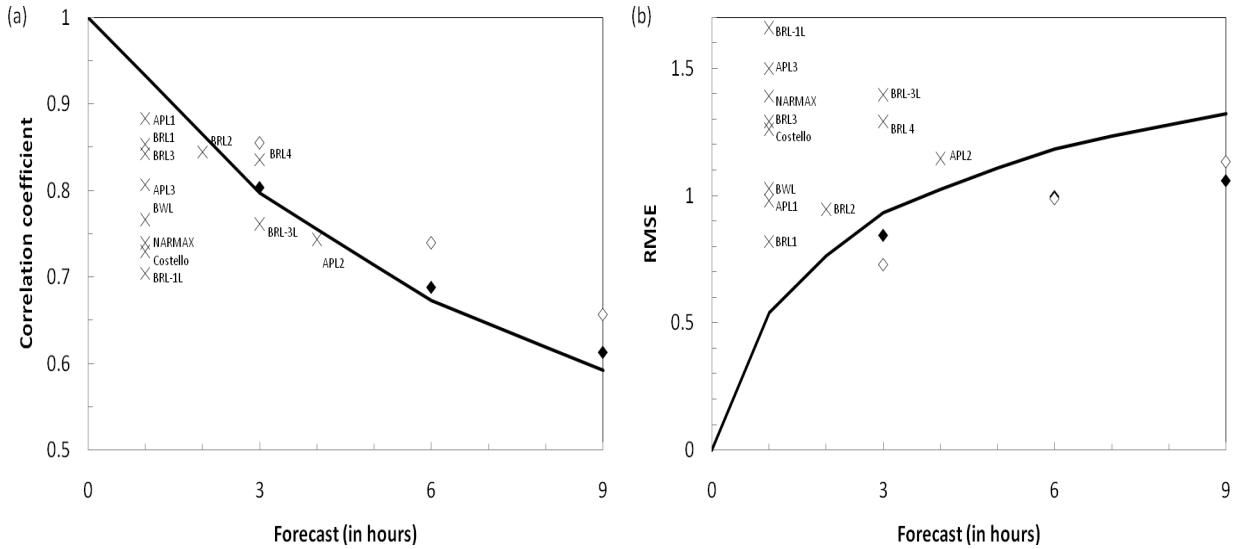

Figure 6 –UKF persistence-only model (solid diamonds) and UKF storm-trigger model (open diamonds) x-hour ahead (a) correlation coefficient and (b) RMSE as a function of x (forecast in hours) for all data. Simple persistence model (line) is for estimated 3-hr smoothed data and all models corrected for interpolation and data set effects.

Fig. 5 reproduces Fig. 3 for the 1998 to 2008 data set and with the UKF models also plotted. Fig. 6 reproduces Fig. 4 with the UKF models also plotted, data interpolation effects removed and the results scaled to a common data set (1933-2008) using the values listed in Table 1. The scaling was done by assuming the percent difference from simple persistence remains constant when using different data sets.

5. CONCLUSIONS

The planetary geomagnetic index displays a high degree of persistence. Previously reported results comparing actual K_p values and forecast values using various forecast models that use sentinel solar wind and IMF data as well as the current K_p have not comprehensively compared the linear correlation and RMSE results to simple persistence and account for effects caused by smoothing and interpolating the K_p data. When this is done, most previously reported forecast models actually perform worse than simple persistence alone. A new measure, the storm onset skill score, is defined such that it equals zero for simple persistence and thus can serve as a true measure of forecast performance.

Models using the unscented Kalman filter (UKF) and various measurement functions were evaluated. Whereas the resulting performance of persistence-only models was only slightly better than simple persistence, the storm-trigger model outperformed all previously published forecast models.

The utility of using the UKF as the engine behind a forecast model is clearly demonstrated and opens up the possibility of incorporating a host of other inputs to the model and exploring the use of other state and measurement functions. Finally, the UKF can be used to forecast other geomagnetic indices as well.

6. REFERENCES

1. Wing, S., J. R. Johnson, J. Jen, C.-I. Meng, D. G. Sibeck, K. Bechtold, J. Freeman, K. Costello, M. Balikhin, and K. Takahashi (2005), Kp forecast models, *J. Geophys. Res*., 110, Issue A4, CiteID A04203

2. Bala, R., P. H. Reiff, and J. E. Landivar (2009), Real-time prediction of magnetospheric activity using the Boyle Index, *Space Weather*, 7, S04003, doi:10.1029/2008SW000407.

3. Julier, S. G., and J. K. Uhlmann (1997), A new extension of the Kalman filter to nonlinear systems, *Proceedings of SPIE: The International Society for Optical Engineers*, Vol. 3068, 182-193

4. van der Merwe, R., and E.A Wan (2001), The square root unscented Kalman filter for state and parameter-estimation, *2001 IEEE International Conference on Acoustics, Speech, and Signal Processing*, Vol. 6, 3461-3464

5. Crassidis, J. L., and F. L. Markley (2003), Unscented filtering for spacecraft attitude estimation, *Journal of Guidance, Control, and Dynamics*, Vol. 26, No. 4, pp. 536-542

6. Jah, M. K., Lisano, M. E., II, Born, G.H., and Axelrad, P. (2008), Mars aerobraking spacecraft state estimation by processing inertial measurement unit data, *Journal of Guidance, Control, and Dynamics*, Vol. 31, No. 6, pp. 1802-1813

7. Wetterer, C. J., and M. K. Jah (2009), Attitude estimation from light curves, *Journal of Guidance, Control, and Dynamics*, Vol. 32, No. 5, pp. 1648-1651

8. Costello, K.A. (1997), Moving the Rice MSFM into a real-time forecast model using solar wind driven forecast models, *PhD. Dissertation, Rice University, Houston, TX*.

9. Balikhin, M. A., O. M. Boaghe, S. A. Billings, and H. St C. K. Alleyne (2001), Terrestrial magnetosphere as a nonlinear resonator, *Geophys. Res. Lett., 28*, 1123-1126.

10. Boberg, F., P. Wintoft, and H. Lundstedt (2000), Real-time Kp prediction from solar wind data using neural networks, *Phys. Chem. Earth*, 25, 275.